Journal of Hazardous Materials B128 (2006) 175–181

Journal of Hazardous Materials

www.elsevier.com/locate/jhazmat

Effect of heating temperature on the sintering characteristics of sewage sludge ash

Kae-Long Lin [a,*], Kung-Yuh Chiang [b], Deng-Fong Lin [c]

[a] *Department of Environmental Engineering, National I-Lan University, 1 Sec. 1, Shen-Lung Road, I-Lan City 260, Taiwan, ROC*

[b] *Department of Environmental Engineering and Science, Feng-Chia University, Tai-Chung 407, Taiwan, ROC*

[c] *Department of Civil and Ecological Engineering, I-Shou University, Kaohsiung County 840, Taiwan, ROC*

Received 4 March 2005; received in revised form 29 July 2005; accepted 30 July 2005
Available online 8 September 2005

Abstract

This study investigated and analyzed the effects of the heating temperature on the properties of the sintered sewage sludge ash. The results indicated that the water absorption rate of the sintered sewage sludge ash samples decreased when the firing temperature was increased from 800 to 900 °C. When the heating temperature reached 1000 °C, the absorption rate decreased significantly. The bulk density of the sewage sludge ash samples increased by 2.3 g/cm^3 when the heating temperature was increased from 900 to 1000 °C, indicating that the densification was affected by heating. The porosity of the sintered sewage sludge ash samples ranged from 36% to 39% when the heating temperature ranged from 600 to 900 °C. The least porosity occurred at 1000 °C; the sintered samples were well densified. When the temperature was between 900 and 1000 °C, the strength appeared to increase significantly, reaching 2040 kgf/cm^2, implying an advance in densification due to sintering. The SEM observations were in general agreement with the trends shown by the density data.

Keywords: Sintering; Porosity; Sewage sludge ash; SEM observation

1. Introduction

There are more than 500,000 tonnes of sewage sludge ashes (SSA) generated in Taiwan annually. Its treatment/disposal and environmental impact have become a major public concern. In addition, the annual consumption of natural resources, such as aggregates and other raw materials for producing cement, is also substantial. The discrepancy between supply and demand, as well as excessive mining has resulted in a substantial reduction of natural resources. The recovery and recycling of the certain inorganic residues from construction materials can mitigate the extent of the problem by slowing the consumption rate of natural resources, and the excessive generation of wastes that requires disposal.

SSA, which contains inorganic components, including Al_2O_3, SiO_2 and in flux (i.e., Fe_2O_3, FeO, CaO, MgO, Na_2O, and K_2O), has been used in construction materials to improve certain properties [1]. It has been used in producing cement mortars [2]; concrete mixtures [3]; bricks [4]; as fine aggregate in mortars [5]; asphalt paving mixes [6]; ceramic materials [7]. The control of the initial SSA composition and the application of a suitable heat treatment allow for the formation of various crystalline phases resulting in desirable properties.

In this study, SSA was sintered and formed using conventional powder processes, ball milling, powder compaction and heating. The purpose of the research was to

* Corresponding author. Tel.: +886 3 9357400x749; fax: +886 3 9367642/59674.
E-mail address: kllin@niu.edu.tw (K.-L. Lin).

0304-3894/$ – see front matter © 2005 Elsevier B.V. All rights reserved.
doi:10.1016/j.jhazmat.2005.07.051

better understand the effect of the varying heating temperature on the strength, bulk density, water absorption, porosity, mineralogy and microstructure of the sintered SSA samples.

2. Materials and methods

2.1. Materials

A dewatered sludge cake sample was heated in a brick-firing kiln at a temperature of 900 °C for 1 h [8]. The ashes were then pulverized with a ball mill until they could pass through a 150 μm sieve. The dried and homogenized ashes were then stored in a desiccator until testing.

2.2. Preparation of compacted sintered SSA samples

The prepared SSA samples were oven-dried at 105 °C for 24 h and ground in a ball mill to form fine powders suitable for pressing. The ashes were compacted at 3.5 MPa to form cylindrical specimens (1.2 cm in diameter and 1.3 cm in height), which were then desiccated before testing. The compacted SSA specimens were put in a platinum plate and burnt in an electrically heated furnace, using a ramp rate of 5 °C/min. The samples were then sintered at temperatures between 600 and 1000 °C, for a time period between 30 and 240 min. After the heating, the samples were cooled rapidly to room temperature and then stored in a desiccator for subsequent analyses of the physical properties and for leachability testing.

2.3. Characterization of sintered specimens

The chemical composition and physical characteristics of the SSA pellets and sintered products were analyzed. The SSA samples were digested using $HNO_3/HClO_4/HF$ according to USEPA SW3050 and then analyzed with inductively coupled plasma atomic emission spectroscopy (ICP-AES) for its major elements. Estimation of the mechanical quality of the samples was obtained by performing the crushing strength tests, as reported in Ref. [9]. In this test, an oven-dried sample was placed in a steel cylinder with an internal diameter of 57 mm and a height of 87 mm. The samples were filled in the cylinder to an upper incision mark, and then covered and pressed down by a steel puncheon, until the upper level of the SSA sample was reduced by a prescribed distance. The crushing strength value was calculated as the ratio between the load and the cross-sectional area of the cylinder, in stress units. The SW846-1311 method, toxicity characteristic leaching procedure (TCLP), was used for heavy metal determination. The weight loss and Absorption testing were measured using the NIEA R204.00T method and ASTM C556, respectively.

The following formulae were used in computing the weight loss, 24 h absorption rate and bulk density of sintered SSA specimens:

$$\begin{aligned}\text{weight loss} = {} & \{\text{weight of SSA specimen before firing} \\ & - \text{weight of SSA specimen after firing}\} \\ & /\text{weight of SSA specimen before firing} \end{aligned} \quad (1)$$

$$\begin{aligned}&\text{24 h absorption rate} \\ &= \{\text{24 h saturated surface-dry weight of SSA specimen} \\ &\quad - \text{dry weight of SSA specimen}\} \\ &\quad /\text{dry weight of SSA specimen}\end{aligned} \quad (2)$$

$$\begin{aligned}&\text{bulk density} \\ &= \text{dry weight of SSA specimen}/ \\ &\quad \{\text{saturated surface dry weight of SSA specimen} \\ &\quad - \text{immersed weight of SSA specimen}\}\end{aligned} \quad (3)$$

A Quantachrome Autoscan Mercury Intrusion Porosimeter (MIP) was used with intrusion pressures up to 60,000 psi. By using the Washburn equation, with $p = -(2\gamma \cos\theta/r)$, the pore volume ($V$) and the corresponding radius (r) could be synchronously plotted by an X–T plotter. The wetting angle of mercury was assumed to be $\theta = 140°$. In this equation, p, γ, r and θ, stand for the applied pressure, surface tension, pore radius and wetting angle, respectively. The crystalline phases present in the sintered SSA samples were determined by X-ray diffraction (XRD, Seimens FTS-40) using 30 mA and 40 kV Cu Kα radiation. The crystalline phases were identified by comparing the intensities and the positions of the Bragg peaks with the data files of the Joint Committee on Powder Diffraction Standards (JCPDS). A Hitachi S-800 scanning electron microscope was used for SEM observation and crystal structural determination.

3. Results and discussion

3.1. Characterization of sewage sludge ash and sintered SSA samples

The chemical compositions of the sludge ash are shown in Table 1. According to ICP-AES analysis, the sludge ash consists of SiO_2, Al_2O_3, and P_2O_5 as the major components, with percentages of 46.27%, 14.12% and 17.75%, respectively. The next most abundant components were Fe_2O_3 (7.46%), CaO (4.80%), MgO (2.01%) and K_2O (1.46%).

Fig. 1 shows the speciation of the components in the sewage sludge ash, as identified by the XRD techniques. The major components identified were quartz (SiO_2), P_2O_5 and Fe_2O_3. The heavy metal leaching concentration of the sludge ash and sintered samples are presented in Table 2. As shown in this table, they are all meeting Taiwan EPA's regulatory requirements.

Table 1
Chemical composition and heavy metals in the sludge ash

Composition	Sludge ash
SiO_2 (wt.%)	46.27 ± 2.1
Al_2O_3 (wt.%)	14.12 ± 1.9
Fe_2O_3 (wt.%)	7.46 ± 0.2
CaO (wt.%)	4.80 ± 0.3
MgO (wt.%)	2.01 ± 0.1
K_2O (wt.%)	1.46 ± 0.1
TiO_2 (wt.%)	0.09 ± 0.0
P_2O_5 (wt.%)	17.75 ± 0.3
Pb (mg/kg)	199.4 ± 4.3
Cd (mg/kg)	8.9 ± 0.1
Zn (mg/kg)	2236 ± 28.6
Cr (mg/kg)	75.7 ± 3.3
Cu (mg/kg)	432.6 ± 9.3

3.2. Effect of sintering temperature on the physical properties of sintered sewage sludge ash

3.2.1. Weight loss of the sintered SSA samples

The weight loss of the SSA pellets after sintering might be due to the release of gases via the conversion of organic residues, the mineral decomposition, or the vaporization of volatile metals in the SSA samples during the sintering process. The quantity and the time of the release can affect the microstructure of the sintered SSA pellets, and thus the strength of the resulting products. The weight losses of SSA samples sintered at various heating temperatures and for various time durations, are shown in Fig. 2. It can be observed from this figure that, with the heating temperature increas-

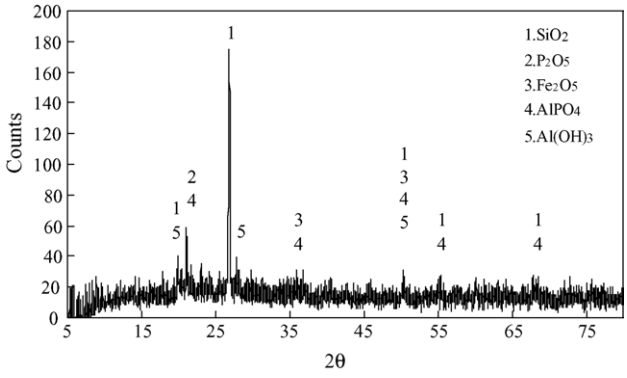

Fig. 1. XRD pattern of sewage sludge ash.

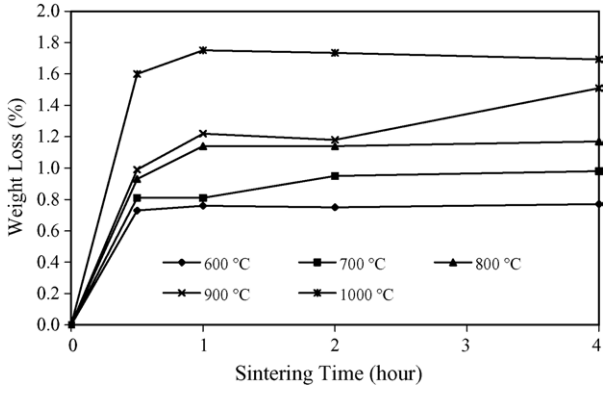

Fig. 2. Effect of heating temperature on the weight loss of SSA sintered samples.

Table 2
TCLP concentration of sewage sludge ash and sintered samples

	Pb (mg/L)	Cd (mg/L)	Cr (mg/L)	Cu (mg/L)	Zn (mg/L)
Sludge ash	ND[a]	0.03 ± 0.01	ND[b]	0.51 ± 0.05	7.04 ± 0.32
600 °C					
1 h	ND	0.03 ± 0.00	ND	0.40 ± 0.03	5.50 ± 0.29
2 h	ND	0.03 ± 0.00	ND	0.40 ± 0.03	5.49 ± 0.15
3 h	ND	0.03 ± 0.00	ND	0.40 ± 0.03	5.42 ± 0.29
700 °C					
1 h	ND	0.03 ± 0.00	ND	0.43 ± 0.01	4.96 ± 0.07
2 h	ND	0.03 ± 0.01	ND	0.37 ± 0.05	5.01 ± 0.05
3 h	ND	0.02 ± 0.00	ND	0.36 ± 0.01	4.87 ± 0.07
800 °C					
1 h	ND	0.02 ± 0.00	ND	0.39 ± 0.04	5.04 ± 0.40
2 h	ND	0.02 ± 0.00	ND	0.40 ± 0.03	4.55 ± 0.39
3 h	ND	0.02 ± 0.00	ND	0.40 ± 0.01	4.54 ± 0.29
900 °C					
1 h	ND	0.02 ± 0.00	ND	0.61 ± 0.07	2.95 ± 0.46
2 h	ND	0.03 ± 0.00	ND	0.57 ± 0.04	3.01 ± 0.25
3 h	ND	0.04 ± 0.01	ND	0.55 ± 0.04	2.97 ± 0.23
1000 °C					
1 h	ND	0.03 ± 0.00	ND	0.54 ± 0.05	2.95 ± 0.36
2 h	ND	0.02 ± 0.00	ND	0.57 ± 0.04	2.82 ± 0.32
3 h	ND	0.03 ± 0.00	ND	0.50 ± 0.02	2.55 ± 0.16
Regulation thresholds	5.0	1.0	5.0	15.0	–

[a] Pb < 0.016 mg/L.
[b] Cr < 0.014 mg/L.

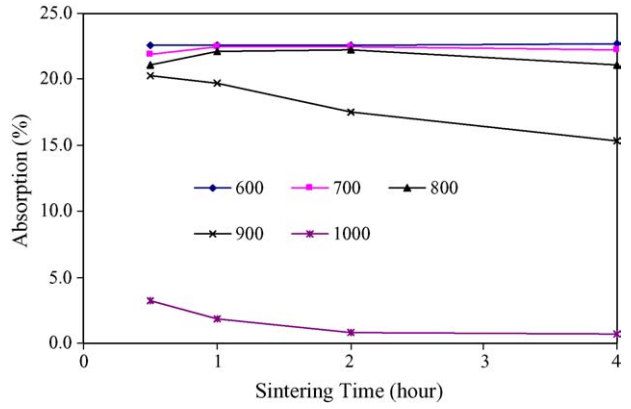

Fig. 3. Effect of heating temperature on the 24 h absorption rate of SSA sintered samples.

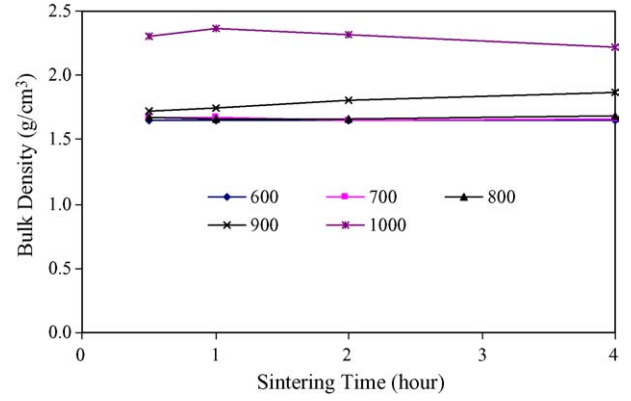

Fig. 4. Effect of heating temperature on the bulk density of SSA sintered samples.

ing from 600 to 1000 °C, the weight loss, suggesting that the weight loss was probably due to the oxidation of organic residues in the SSA.

3.2.2. *Water absorption of the sintered SSA samples*

The water absorption of the sintered SSA samples was determined by measuring the apparent weight increase of a dried sample after it was immersed in water for 24 h (defined

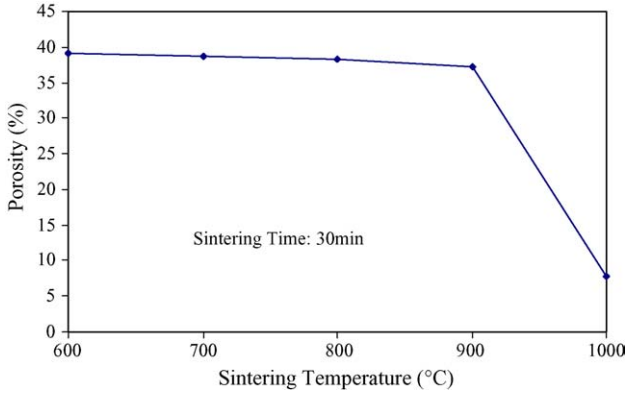

Fig. 5. Effect of heating temperature on the porosity of SSA sintered samples for 30 min.

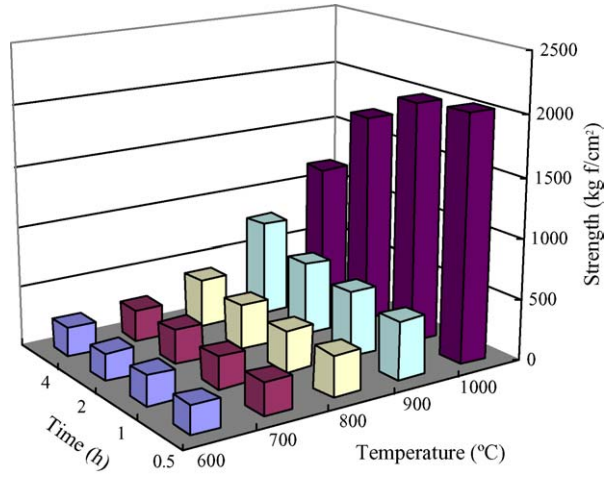

Fig. 6. Effect of heating temperature on the strength of sintered SSA samples.

as the 24 h absorption rate). Fig. 3 shows the variation in the 24 h absorption weight as functions of various heating temperatures and times. The results of the 24 h absorption demonstrated that a reduction of the open, water accessible porosity occurred when the heating temperature was increased from 600 to 800 °C. The absorption ranged from 20% to 23%. However, the water absorption of the sintered SSA samples decreased when the heating temperature increased from 800 to 900 °C. When the heating temperature reached 1000 °C, the absorption rate decreased significantly (to as low as 3%). The results are in good agreement with Cheeseman et al. results [7]. It is suggested that the reduction in water absorption was due to the decreasing pore volume and the effects of densification. Both the 3 and 4 h sintered SSA samples heated

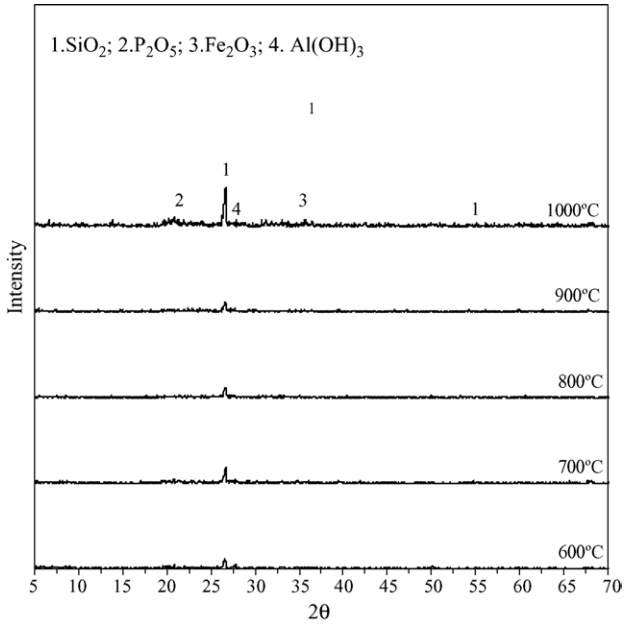

Fig. 7. X-ray diffraction of SSA sintered samples at 600–1000 °C for 30 min.

at 1000 °C were effectively impermeable, with absorption values of less than 0.3%.

3.2.3. Bulk density of the sintered SSA samples

Fig. 4 shows the correlations between the bulk density and the heating temperature, for both the raw SSA and the sintered SSA samples. When the SSA samples were heated from 600 to 900 °C, the bulk density increased (ranging from 1.6 to 1.7 g/cm^3). The bulk density of the SSA samples increased by 2.3 g/cm^3 when the heating temperature was raised from 900 to 1000 °C, indicating that densification was caused by heating. The 1 h sintered samples had a maximum density of 2.43 g/cm^3, which was achieved by heating at 1000 °C for 1 h. The maximum density of 2.37 g/cm^3 was achieved by heating at 1000 °C. The results are in good agreement with Cheeseman et al. results [7]. Samples heated at lower temperatures had significantly lower densities, compared to the corresponding 1 h sintered samples. Heating at 1000 °C for 4 h resulted in a slight reduction in density to 2.23 g/cm^3.

3.2.4. Porosity and pore size distribution

The porosity of SSA samples sintered at temperatures ranging from 600 to 1000 °C for 30 min were measured with a mercury intrusion porosimeter. The results are shown in Fig. 5. The porosity varied with the heating temperature, which indicates that increasing in sintering temperature

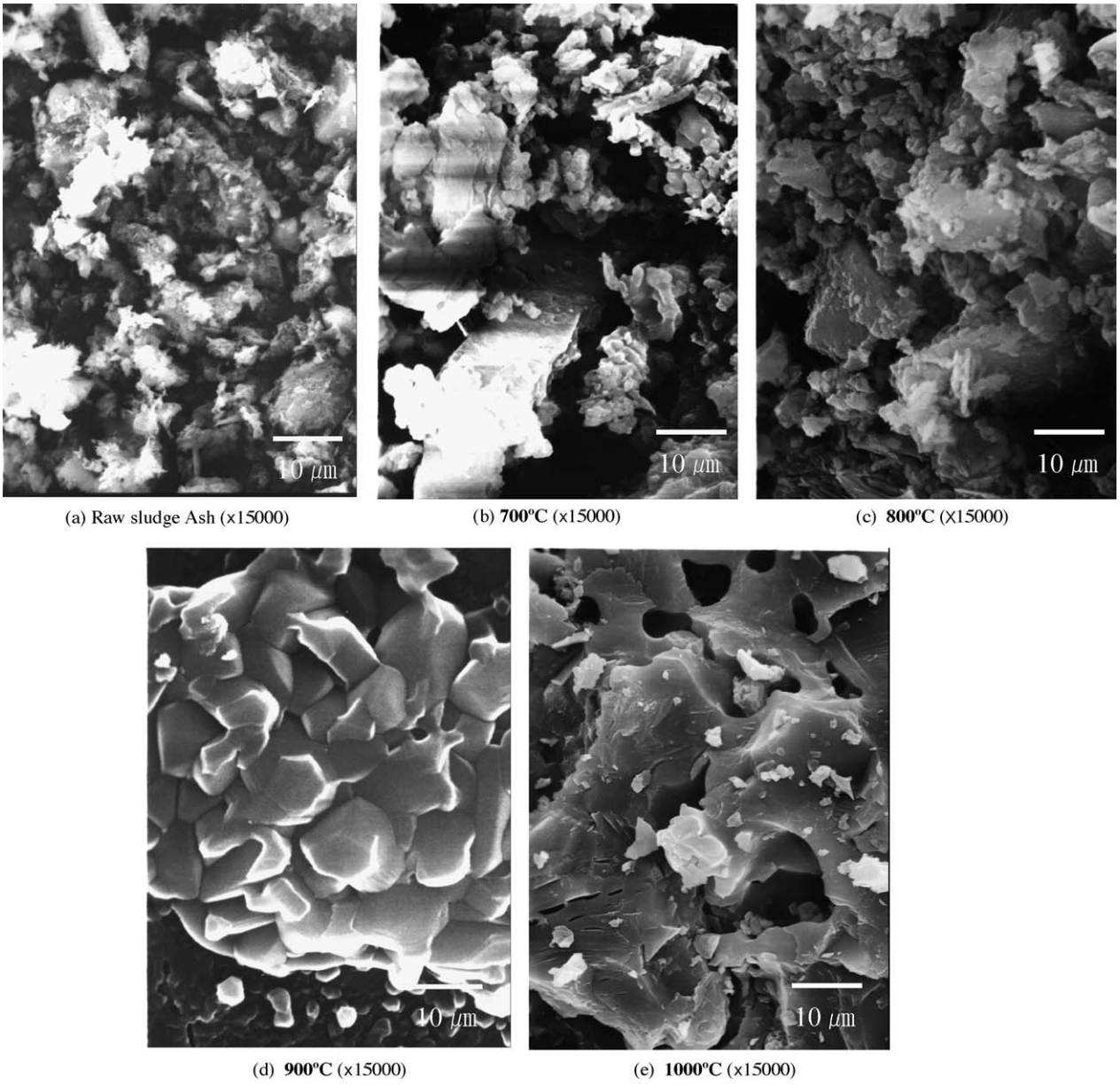

Fig. 8. Scanning electron micrograph images of sewage sludge ash sintered at 700–1000 °C for 30 min.

resulted in reduced, thereby decreasing the porosity of the sintered samples. The porosity ranged from 36% to 39% when the sintering temperature was between 600 and 900 °C. The least porosity occurred at 1000 °C, where the sintered samples were well dandified. Changes in the density, porosity and water absorption with heating temperature are believed to be a result of the softening of the glassy phase in the system, along with a concurrent evolution of gas at high temperatures. For example, the reduction of Fe^{3+} to Fe^{2+} involves the release of O_2 [10]. On the other hand, although the effect of the volume–temperature relationship is extremely small [11], the amorphous structure occupies a larger specific volume than the crystalline structure. When glass is heated at a certain temperature, its volume increases and crystallization occurs, resulting in a decrease in the specific volume [12].

3.2.5. Crushing strength of the sintered SSA samples

The strength test results of SSA samples sintered at temperatures from 600 to 1000 °C, and for the various heating temperature and times, are shown in Fig. 6. In general, the strength of the SSA samples were affected by several interrelated factors, such as the porosity, the pore size and distribution, the mineral species in the SSA, speciation variation during heating and densification effects due to sintering. In the experiments the strength increased with increasing heating temperature. Between 900 and 1000 °C, the strength appeared to increase significantly, reaching 2040 kgf/cm^2, implying an advance in densification due to sintering.

3.3. Microstructural characterisation

XRD data for 30 min sintered samples heated at different temperatures are shown in Fig. 7. $AlPO_4$, originally in the SSA, were not detected in sintered samples. The major peak at $2\theta = 26.5^\circ$ was quartz. In comparison, the intensities of the peaks associated with $AlPO_4$ significantly decreased as heating temperature was increased. Sintered SSA samples at 1000 °C samples were also compared to raw SSA. The results indicated that they contained less amorphous silicate glass.

3.4. SEM observation of sintered SSA samples

Fig. 8(a)–(e) shows the microstructure of sintered ash examined by SEM photographic techniques. The SEM observations showed that the pore structure became more compact due to the increasing sintering temperature. The observations clearly showed the particulate nature of the sintered SSA particles in the raw sludge ash (Fig. 8(a)), whereas in the sintered samples, they become more fused. On other hand, sinter bonding is evident by cohesive necks growing at the particle contact points. In Fig. 8(b), the fractured surface of the sample sintered at 700 °C is rough and granular. Fig. 8(c) illustrates SSA sintered at 800 °C, clearly showing the advance in densification and neck growth between the ash particles. However, in Fig. 8(d) the SSA samples sintered at 900 °C show clear neck growth between the particles but that the particle size is much greater than that of the original untreated ash, suggesting the occurrence of defect neck growth. The slight expansion of the sample that occurred when sintered at 1000 °C is clearly associated with the formation of a significant volume of approximately spherical pores, as can be seen in Fig. 8(e). These are believed to be a result of the softening of the glassy phase present in the ash, along with a simultaneous evolution of gas at 1000 °C. The SEM observations are in general agreement with the trends shown by the density data.

4. Conclusions

This study has demonstrated that sewage sludge ash can be recycled by heat-treatment for use as construction materials. The results are outlined as follows:

1. The sludge ash consists of SiO_2, Al_2O_3, Fe_2O_3, and P_2O_5 as the major components.
2. The heavy metal leaching concentration of the sludge ash and sintered samples all met Taiwan EPA's regulatory thresholds.
3. The water absorption of sintered SSA samples decreased as the heating temperature increased.
4. The porosity varied with the heating temperature, which indicates that increasing the sintering temperature would reduce the pore volume, thereby decrease the porosity of the sintered samples.
5. The bulk density of the SSA samples increased when the temperature was increased resulting in densified structure that is associated with water absorption.

References

[1] R. Cenni, B. Janisch, H. Spliethoff, K.R.G. Hein, Legislative and environmental issues on the use of ash from coal and municipal sewage sludge co-firing as construction material, Waste Manage. 21 (2001) 17–31.
[2] J. Monzo', J. Paya', M.V. Borrachero, I. Girbe's, Reuse of sewage sludge ashes (SSA) in cement mixtures: the effect of SSA on the workability of cement mortars, Waste Manage. 23 (2003) 373–381.
[3] J.N. Diet, P. Moszkowicz, D. Sorrentino, Behaviour of ordinary Portland cement during the stabilization/solidification of synthetic heavy metal sludge: macroscopic and microscopic aspects, Waste Manage. 18 (1998) 17–24.
[4] J.E. Alleman, N.A. Berman, Constructive sludge management: biobrick, J. Environ. Eng. Div. ASCE 110 (1984) 301–311.
[5] J.I. Bhatty, J.K. Reid, Compressive strength of municipal sludge ash mortars, ACI Mater. 86 (1989) 394–400.
[6] M.H. Al Sayed, I.M. Madany, A.R.M. Buali, Use of sewage sludge ash in asphaltic paving mixes in hot regions, Constr. Build. Mater. 9 (1995) 19–23.
[7] C.R. Cheeseman, C.J. Sollars, S. McEntee, Properties, microstructure and leaching of sintered sewage sludge ash, Res. Conserv. Rec. 40 (2003) 13–25.

[8] J.H. Tay, W.K. Yip, K.Y. Show, Clay-blended sludge as lightweight aggregate concrete material, J. Environ. Eng. Div. ASCE 117 (1991) 834–844.
[9] R. Wasserman, A. Bentur, Effect of lightweight bottom ash aggregate microstructure on the strength of concretes, Cement Concrete Res. 27 (1997) 525–537.
[10] V.M. Sglavo, R. Campostrini, S. Maurina, G. Carturan, M. Monagheddu, G. Budroni, G. Cocco, Bauxite 'red mud' in the ceramic industry. Part 1. Thermal behaviour, J. Eur. Ceram. Soc. 20 (2000) 235–244.
[11] R.C. Ropp, Inorganic Polymeric Glasses, Elsevier Science Publishers, New York, NY, 1992.
[12] J. Zarzycki, Glasses and the Vitreous State, Cambridge University Press, New York, NY, 1991.